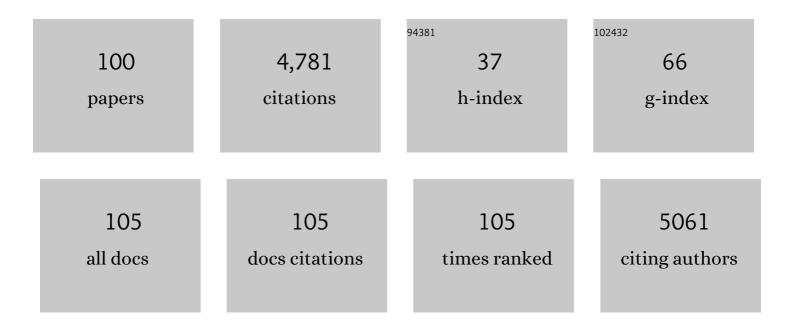
List of Publications by Year in descending order

Source: https://exaly.com/author-pdf/6412673/publications.pdf Version: 2024-02-01



EMDE EDDEM

#	Article	IF	CITATIONS
1	Upcycling process of transforming waste coffee into spherical graphene by flash pyrolysis for sustainable supercapacitor manufacturing with virgin graphene electrodes and its comparative life cycle assessment. Biomass Conversion and Biorefinery, 2024, 14, 1073-1088.	2.9	5
2	ZnO and reduced graphene oxide electrodes for all-in-one supercapacitor devices. Nanoscale, 2022, 14, 3269-3278.	2.8	70
3	Spectroscopic Probing Of Mn-Doped ZnO Nanowires Synthesized via a Microwave-Assisted Route. Journal of Physical Chemistry C, 2022, 126, 4229-4240.	1.5	14
4	EPR investigation of point defects in HfB2 and their roles in supercapacitor device performances. Applied Physics Letters, 2022, 120, .	1.5	19
5	Solar-assisted all-solid supercapacitors using composite nanostructures of ZnO nanowires with GO and rGO. Journal of Materials Chemistry C, 2022, 10, 10748-10758.	2.7	18
6	Photo-supercapacitors based on nanoscaled ZnO. Scientific Reports, 2022, 12, .	1.6	28
7	Why <scp><i>P2X</i></scp> must be the part of the energy solution?. Environmental Progress and Sustainable Energy, 2021, 40, e13545.	1.3	11
8	About defect phenomena in ZnO nanocrystals. Nanoscale, 2021, 13, 9160-9171.	2.8	73
9	ZnO and MXenes as electrode materials for supercapacitor devices. Beilstein Journal of Nanotechnology, 2021, 12, 49-57.	1.5	46
10	Unveiling the presence of mixed oxidation states of Europium in Li _{7+Î′} Eu _x La _{3â^îÎ′} Zr _{2â^îÎ′} O _{12â^îÎ′} garnet and its impact on the Liâ€ion conductivity. Journal of the American Ceramic Society, 2021, 104, 4257-4271.	1.9	10
11	Building an Iron Chromophore Incorporating Prussian Blue Analogue for Photoelectrochemical Water Oxidation. Chemistry - A European Journal, 2021, 27, 8966-8976.	1.7	9
12	Building an Iron Chromophore Incorporating Prussian Blue Analogue for Photoelectrochemical Water Oxidation. Chemistry - A European Journal, 2021, 27, 8890-8890.	1.7	0
13	Defect-induced B4C electrodes for high energy density supercapacitor devices. Scientific Reports, 2021, 11, 11627.	1.6	15
14	Low-Temperature Surface Phase Transitions in Multiferroic BiFeO ₃ Nanocrystals Probed via Electron Paramagnetic Resonance. Journal of Physical Chemistry C, 2021, 125, 24596-24604.	1.5	7
15	Efficiency enhancement in photoelectrochemical water splitting: Defect passivation and boosted charge transfer kinetics of zinc oxide nanostructures via chalcopyrite/chalcogenide mix sensitization. Physical Review Materials, 2021, 5, .	0.9	5
16	Synthesis and Assembly of Zinc Oxide Microcrystals by a Lowâ€Temperature Dissolution–Reprecipitation Process: Lessons Learned About Twin Formation in Heterogeneous Reactions. Chemistry - A European Journal, 2020, 26, 9319-9329.	1.7	1
17	Electrical properties, EPR analyses and defect chemistry of Mn-doped 0.675PMN-0.325PT piezoceramics. Ceramics International, 2020, 46, 28980-28986.	2.3	10
18	Coreâ€crown Quantum Nanoplatelets with Favorable Typeâ€l Heterojunctions Boost Charge Separation and Photocatalytic NO Oxidation on TiO ₂ . ChemCatChem, 2020, 12, 6329-6343.	1.8	16

#	Article	IF	CITATIONS
19	Tailoring morphology to control defect structures in ZnO electrodes for high-performance supercapacitor devices. Nanoscale, 2020, 12, 16162-16172.	2.8	99
20	Synergy of nano-ZnO and 3D-graphene foam electrodes for asymmetric supercapacitor devices. Nanoscale, 2020, 12, 12790-12800.	2.8	65
21	Applications of Supercapacitors in Space Vehicles and Interplanetary Devices. , 2020, , .		0
22	Capacitive behaviour of nanocrystalline octacalcium phosphate (OCP) (Ca ₈ H ₂ (PO ₄) ₆ ·5H ₂ O) as an electrode material for supercapacitors: biosupercaps. Nanoscale, 2019, 11, 18375-18381.	2.8	41
23	Layer-by-Layer Grown Electrodes Composed of Cationic Fe ₃ O ₄ Nanoparticles and Graphene Oxide Nanosheets for Electrochemical Energy Storage Devices. Journal of Physical Chemistry C, 2019, 123, 3393-3401.	1.5	34
24	Current progress achieved in novel materials for supercapacitor electrodes: mini review. Nanoscale Advances, 2019, 1, 2817-2827.	2.2	591
25	Oxidative Fluorination of Cu/ZnO Methanol Catalysts. Angewandte Chemie - International Edition, 2019, 58, 12935-12939.	7.2	13
26	Oxidative Fluorination of Cu/ZnO Methanol Catalysts. Angewandte Chemie, 2019, 131, 13069-13073.	1.6	4
27	Feeling the power: robust supercapacitors from nanostructured conductive polymers fostered with Mn ²⁺ and carbon dots. Nanoscale, 2019, 11, 12804-12816.	2.8	67
28	Superbat: battery-like supercapacitor utilized by graphene foam and zinc oxide (ZnO) electrodes induced by structural defects. Nanoscale Advances, 2019, 1, 2586-2597.	2.2	97
29	High-quality MgB2 nanocrystals synthesized by using modified amorphous nano-boron powders: Study of defect structures and superconductivity properties. AIP Advances, 2019, 9, .	0.6	9
30	Discovery of an Exceptionally Strong Luminescence of Polyethyleneimine‧uperparamagnetic Iron Oxide Nanoparticles. Macromolecular Chemistry and Physics, 2018, 219, 1700563.	1.1	8
31	Synergetic effects of Fe ³⁺ doped spinel Li ₄ Ti ₅ O ₁₂ nanoparticles on reduced graphene oxide for high surface electrode hybrid supercapacitors. Nanoscale, 2018, 10, 1877-1884.	2.8	163
32	Developing intercalation based anode materials for fluoride-ion batteries: topochemical reduction of Sr ₂ TiO ₃ F ₂ <i>via</i> a hydride based defluorination process. Journal of Materials Chemistry A, 2018, 6, 22013-22026.	5.2	27
33	Hardening behavior and highly enhanced mechanical quality factor in (K 0.5 Na 0.5)NbO 3 –based ceramics. Journal of the European Ceramic Society, 2017, 37, 2083-2089.	2.8	42
34	Toward an Understanding of Thin-Film Transistor Performance in Solution-Processed Amorphous Zinc Tin Oxide (ZTO) Thin Films. ACS Applied Materials & Interfaces, 2017, 9, 21328-21337.	4.0	33
35	High-Capacitance Hybrid Supercapacitor Based on Multi-Colored Fluorescent Carbon-Dots. Scientific Reports, 2017, 7, 11222.	1.6	224
36	Defect induced p-type conductivity in zinc oxide at high temperature: electron paramagnetic resonance spectroscopy. Nanoscale, 2017, 9, 10983-10986.	2.8	23

#	Article	IF	CITATIONS
37	Defect Structure of Doped Leadâ€Free 0.9(Bi _{0.5} Na _{0.5})TiO ₃ â^'0.1(Bi _{0.5} K _{0.5})TiO _{ Piezoceramics. Journal of the American Ceramic Society, 2016, 99, 543-550.}	3 1/9 ub>	10
38	Al-doped MgB2 materials studied using electron paramagnetic resonance and Raman spectroscopy. Applied Physics Letters, 2016, 108, .	1.5	23
39	The effect of growing time and Mn concentration on the defect structure of ZnO nanocrystals: X-ray diffraction, infrared and EPR spectroscopy. RSC Advances, 2016, 6, 39511-39521.	1.7	23
40	Competing effects between intrinsic and extrinsic defects in pure and Mn-doped ZnO nanocrystals. Journal of Nanoparticle Research, 2016, 18, 1.	0.8	47
41	Defect Evolution of Nonstoichiometric ZnO Quantum Dots. Journal of Physical Chemistry C, 2016, 120, 25124-25130.	1.5	96
42	Charge transfer and surface defect healing within ZnO nanoparticle decorated graphene hybrid materials. Nanoscale, 2016, 8, 9682-9687.	2.8	74
43	Zinc diketonates as single source precursors for ZnO nanoparticles: microwave-assisted synthesis, electrophoretic deposition and field-effect transistor device properties. Journal of Materials Chemistry C, 2016, 4, 7345-7352.	2.7	17
44	Controlling the exciton energy of zinc oxide (ZnO) quantum dots by changing the confinement conditions. Spectrochimica Acta - Part A: Molecular and Biomolecular Spectroscopy, 2016, 152, 637-644.	2.0	96
45	The effects of passive leg raising and ultrafiltration stopping on blood pressure in hemodialysis patients. International Urology and Nephrology, 2016, 48, 877-882.	0.6	3
46	Effects of MnO doping on the electronic properties of zinc oxide: 406 GHz electron paramagnetic resonance spectroscopy and Newman superposition model analysis. Journal of Applied Physics, 2015, 118, .	1.1	14
47	Electron paramagnetic resonance and Raman spectroscopy studies on carbon-doped MgB2 superconductor nanomaterials. Journal of Applied Physics, 2015, 117, .	1.1	35
48	A microwave molecular solution based approach towards high-κ-tantalum(<scp>v</scp>)oxide nanoparticles: synthesis, dielectric properties and electron paramagnetic resonance spectroscopic studies of their defect chemistry. Physical Chemistry Chemical Physics, 2015, 17, 31801-31809.	1.3	9
49	Electron paramagnetic resonance study of ZnO varistor material. Journal of Physics Condensed Matter, 2014, 26, 115801.	0.7	36
50	Aging in the relaxor and ferroelectric state of Fe-doped (1-x)(Bi1/2Na1/2)TiO3-xBaTiO3 piezoelectric ceramics. Journal of Applied Physics, 2014, 116, .	1.1	58
51	Defect structure of ultrafine MgB2 nanoparticles. Applied Physics Letters, 2014, 105, .	1.5	27
52	Comparative electron paramagnetic resonance investigation of reduced graphene oxide and carbon nanotubes with different chemical functionalities for quantum dot attachment. Applied Physics Letters, 2014, 104, .	1.5	80
53	Microwave power, temperature, atmospheric and light dependence of intrinsic defects in ZnO nanoparticles: A study of electron paramagnetic resonance (EPR) spectroscopy. Journal of Alloys and Compounds, 2014, 605, 34-44.	2.8	133
54	Improved efficiency of bulk heterojunction hybrid solar cells by utilizing CdSe quantum dot–graphene nanocomposites. Physical Chemistry Chemical Physics, 2014, 16, 12251-12260.	1.3	45

#	Article	IF	CITATIONS
55	Local coordination of Fe ³⁺ in ZnO nanoparticles: multi-frequency electron paramagnetic resonance (EPR) and Newman superposition model analysis. Journal of Physics Condensed Matter, 2014, 26, 155803.	0.7	11
56	Microwaveâ€Assisted Synthesis, Characterisation and Dielectric Properties of Nanocrystalline Zirconia. European Journal of Inorganic Chemistry, 2014, 2014, 5554-5560.	1.0	7
57	Mn-substituted spinel Li4Ti5O12 materials studied by multifrequency EPR spectroscopy. Journal of Materials Chemistry A, 2013, 1, 9973.	5.2	74
58	SPACE-CHARGE LAYER, INTRINSIC "BULK" AND SURFACE COMPLEX DEFECTS IN ZnO NANOPARTICLES — A HIGH-FIELD ELECTRON PARAMAGNETIC RESONANCE ANALYSIS. Functional Materials Letters, 2013, 06, 1330004.	0.7	13
59	Molecular precursor derived and solution processed indium–zinc oxide as a semiconductor in a field-effect transistor device. Towards an improved understanding of semiconductor film composition. Journal of Materials Chemistry C, 2013, 1, 2577.	2.7	34
60	Investigation of intrinsic defects in core-shell structured ZnO nanocrystals. Journal of Applied Physics, 2012, 111, .	1.1	100
61	High-Frequency EPR Analysis of MnO ₂ -Doped [Bi _{0.5} Na _{0.5}]TiO ₃ -BaTiO ₃ Piezoelectric Ceramics – Manganese Oxidation States and Materials â€~Hardening'. Ferroelectrics, 2012, 428, 116-121.	0.3	17
62	EPR and photoluminescence spectroscopy studies on the defect structure of ZnO nanocrystals. Physical Review B, 2012, 86, .	1.1	300
63	Influence of reducing atmosphere on the defect chemistry of lead lanthanum zirconate titanate (8/65/35). Solid State Ionics, 2012, 228, 56-63.	1.3	2
64	Local coordination of Fe3+ in Li[Co0.98Fe0.02]O2 as cathode material for lithium ion batteries—multi-frequency EPR and Monte-Carlo Newman-superposition model analysis. Physical Chemistry Chemical Physics, 2011, 13, 9344. tp://www.w3.org/1998/Math/Math/Mc	1.3	18
65	display="inline"> <mml:mrow><mml:mo>(</mml:mo><mml:mn>1</mml:mn><mml:mo>a" </mml:mo>a" xmlns:mml="http://www.w3.org/1998/Math/MathML" display="inline"><mml:msub><mml:mrow /><mml:mn>3</mml:mn></mml:mrow </mml:msub>â€"<mml:math xmlns:mml="http://www.w3.org/1998/Math/MathML"</mml:math </mml:mrow>	x1.1	39
66	display="initial" > chimicmi> xc/mmcmach>Porto < mmcmach xmlns:mml="http://www.w3.org/199 Impact of Defect Structure on 'Bulk' and Nano-Scale Ferroelectrics. , 2011, , .		1
67	Processing of Manganese-Doped [Bi0.5Na0.5]TiO3 Ferroelectrics: Reduction and Oxidation Reactions During Calcination and Sintering. Journal of the American Ceramic Society, 2011, 94, 1363-1367.	1.9	70
68	CuO as a sintering additive for (Bi1/2Na1/2)TiO3–BaTiO3–(K0.5Na0.5)NbO3 lead-free piezoceramics. Journal of the European Ceramic Society, 2011, 31, 2107-2117.	2.8	72
69	Finite size effects in ZnO nanoparticles: An electron paramagnetic resonance (EPR) analysis. Physica Status Solidi - Rapid Research Letters, 2011, 5, 56-58.	1.2	117
70	Defect structure of the mixed ionic–electronic conducting Sr[Ti,Fe]Ox solid-solution system — Change in iron oxidation states and defect complexation. Solid State Ionics, 2011, 184, 47-51.	1.3	35
71	Position of defects with respect to domain walls in Fe3+-doped Pb[Zr0.52Ti0.48]O3 piezoelectric ceramics. Applied Physics Letters, 2011, 98, .	1.5	77
72	Size effects in Fe3+-doped PbTiO3 nanocrystals—Formation and orientation of defect-dipoles. Journal of the European Ceramic Society, 2010, 30, 289-293.	2.8	42

#	Article	IF	CITATIONS
73	FORMATION OF \$({m Ti}'_{m Ti} - V_{m O}^{ullet ullet})^{ullet}\$ DEFECT DIPOLES IN BaTiO3 CERAMICS HEAT-TREATED UNDER REDUCED OXYGEN PARTIAL-PRESSURE. Functional Materials Letters, 2010, 03, 65-68.	0.7	30
74	Effect of Nb-donor and Fe-acceptor dopants in (Bi1/2Na1/2)TiO3–BaTiO3–(K0.5Na0.5)NbO3 lead-free piezoceramics. Journal of Applied Physics, 2010, 108, .	1.1	75
75	Site of incorporation and solubility for Fe ions in acceptor-doped PZT ceramics. Journal of Applied Physics, 2010, 107, .	1.1	26
76	Synthesis, Characterization, Defect Chemistry, and FET Properties of Microwave-Derived Nanoscaled Zinc Oxide. Chemistry of Materials, 2010, 22, 2203-2212.	3.2	117
77	Defect structure in aliovalently-doped and isovalently-substituted PbTiO ₃ nano-powders. Journal of Physics Condensed Matter, 2010, 22, 345901.	0.7	32
78	Defect structure and materials "hardening―in Fe2O3-doped [Bi0.5Na0.5]TiO3 ferroelectrics. Applied Physics Letters, 2010, 97, .	1.5	79
79	Zinc oxide derived from single source precursor chemistry under chimie douce conditions: formation pathway, defect chemistry and possible applications in thin film printing. Journal of Materials Chemistry, 2009, 19, 1449.	6.7	73
80	Formation of magnetic grains in ferroelectric Pb[Zr0.6Ti0.4]O3 ceramics doped with Fe3+ above the solubility limit. Applied Physics Letters, 2009, 94, 142901.	1.5	41
81	Defect structure and formation of defect complexes in Cu2+-modified metal oxides derived from a spin-Hamiltonian parameter analysis. Molecular Physics, 2009, 107, 1981-1986.	0.8	37
82	Defect structure in lithium-doped polymer-derived SiCN ceramics characterized by Raman and electron paramagnetic resonance spectroscopy. Physical Chemistry Chemical Physics, 2009, 11, 5628.	1.3	37
83	Comment on the article: "Preparation and characterisation of nanocrystalline ZnO particles from a hydrothermal process―by Yi Hu and Hung-Jiun Chen, DOI 10.1007/s11051-007-9264-0. Journal of Nanoparticle Research, 2008, 10, 1369-1369.	0.8	0
84	Luminescence of heat-treated silicon-based polymers: promising materials for LED applications. Journal of Materials Science, 2008, 43, 5790-5796.	1.7	46
85	DEFECT STRUCTURE IN "SOFT" (Gd , Fe)-CODOPED PZT 52.5/47.5 PIEZOELECTRIC CERAMICS. Functional Materials Letters, 2008, 01, 7-11.	0.7	15
86	Characterization of (Fe _{Zr,Ti} -V _o ^{ldrldr}) ^{ldr} defect dipoles in (La,Fe)-codoped PZT 52.5/47.5 piezoelectric ceramics by multifrequency electron paramagnetic resonance spectroscopy. IEEE Transactions on Ultrasonics, Ferroelectrics, and Frequency Control, 2008, 55, 1061-1068.	1.7	37
87	Reorientation of (MnTi″â~'VO••)× defect dipoles in acceptor-modified BaTiO3 single crystals: An electror paramagnetic resonance study. Applied Physics Letters, 2008, 93, .	¹ 1.5	111
88	Size Effects in Ferroelectric PbTiO3 Nanomaterials Observed by Multi-Frequency Electron Paramagnetic Resonance Spectroscopy. Journal of Nanoscience and Nanotechnology, 2008, 8, 702-716.	0.9	16
89	Microstructural Characterization of the Manganese Functional Center Site in PbTiO3 Ferroelectrics—Multi-Frequency Electron Paramagnetic Resonance and Newman Superposition Model Analysis. Ferroelectrics, 2008, 363, 39-49.	0.3	18
90	Local symmetry-reduction in tetragonal (La,Fe)-codoped Pb[Zr _{0.4} Ti _{0.6}]O ₃ piezoelectric ceramics. Physica Scripta, 2007, T129, 12-16.	1.2	30

#	Article	IF	CITATIONS
91	Study of the tetragonal-to-cubic phase transition in PbTiO3nanopowders. Journal of Physics Condensed Matter, 2006, 18, 3861-3874.	0.7	55
92	Dielectric Investigations and Theoretical Calculations of Size Effect in Lead Titanate Nanocrystals. Materials Science Forum, 2006, 514-516, 235-239.	0.3	3
93	Dielectric investigations and theoretical calculations of size effect in lead titanate nanocrystals. IEEE Transactions on Ultrasonics, Ferroelectrics, and Frequency Control, 2006, 53, 2270-2274.	1.7	5
94	Size effects in chromium-doped PbTiO3 nanopowders observed by multi-frequency EPR. Magnetic Resonance in Chemistry, 2005, 43, S174-S182.	1.1	22
95	Incorporation of chromium into hexagonal barium titanate: an electron paramagnetic resonance study. Journal of Physics Condensed Matter, 2005, 17, 2763-2774.	0.7	19
96	Size Effects in BaTiO3Nanopowders Studied by EPR and NMR. Ferroelectrics, 2005, 316, 43-49.	0.3	11
97	Preparation of lead titanate ultrafine powders from combined polymerisation and pyrolysis route. Journal of Materials Science, 2003, 38, 3211-3217.	1.7	31
98	Multi-frequency EPR studyof Cr3+ doped lead titanate (PbTiO3) nanopowders. Physica Status Solidi (B): Basic Research, 2003, 239, R7-R9.	0.7	25
99	Preparation of Nanocrystalline BaTiO3Characterized by in Situ X-ray Absorption Spectroscopy. Journal of Physical Chemistry B, 2001, 105, 3415-3421.	1.2	28
100	Size Effects in Ba(Pb)TiO3 Nanopowders by EPR and NMR. , 0, , 351-361.		0